



HAL
open science

Analyzing the effect of dilatation on the velocity gradient tensor using a model problem

Michel Gonzalez

► **To cite this version:**

Michel Gonzalez. Analyzing the effect of dilatation on the velocity gradient tensor using a model problem. SN Applied Sciences, 2020, 2 (11), 10.1007/s42452-020-03513-4 . hal-03043270

HAL Id: hal-03043270

<https://hal.science/hal-03043270>

Submitted on 7 Dec 2020

HAL is a multi-disciplinary open access archive for the deposit and dissemination of scientific research documents, whether they are published or not. The documents may come from teaching and research institutions in France or abroad, or from public or private research centers.

L'archive ouverte pluridisciplinaire **HAL**, est destinée au dépôt et à la diffusion de documents scientifiques de niveau recherche, publiés ou non, émanant des établissements d'enseignement et de recherche français ou étrangers, des laboratoires publics ou privés.

Analyzing the effect of dilatation on the velocity gradient tensor using a model problem

M. Gonzalez

Received: date / Accepted: date

Abstract The effect of variable mass density on the velocity gradient tensor is addressed by means of a model problem. An equation system for both the velocity gradient and the pressure Hessian tensor is solved assuming a realistic expansion rate. The model results show the evolution of the velocity gradient tensor as the density front is approached and are relevant to the physics of flame fronts.

Keywords Variable mass density · Velocity gradient tensor · Pressure Hessian · Strain properties · Flame fronts

1 Introduction

The influence of local mass density variations upon the properties of the velocity gradient tensor is especially significant in compressible flows or in reacting flows with heat release. Intensity and orientation of both strain and vorticity may be altered, which eventually plays on the growth rate and alignment of scalar gradients. Through the velocity gradient, mass density gradients may thus influence the mixing process, a phenomenon addressed in compressible turbulence [1, 2] and in turbulent flames [3–5].

Such indirect effects often stem from an intricate interaction. For instance, there is now some evidence that, to a large extent, the small-scale physics of turbulent flames is governed by the interplay of the respective gradients of velocity, concentration, and mass density. Explaining the resulting phenomena may thus require, as a first step, analyzing each underlying mechanism separately. The present work is based on this kind of approach.

The basic model problem is the evolution of the velocity gradient tensor undergoing a given expansion rate. This is a one-way coupling in which heat release, for instance, is forced in a restricted flow region, and subsequently affects the velocity gradient properties. The equation system for the velocity gradient tensor,

M. Gonzalez
CNRS, UMR 6614 CORIA, Site universitaire du Madrillet
76801 Saint-Etienne du Rouvray, France
E-mail: michel.gonzalez@coria.fr

including the enhanced homogenized Euler equation (EHEE) model of Suman and Girimaji [6] for the pressure Hessian tensor, is solved in a two-dimensional Euler flow (Sect. 2). The evolution of strain structure is analyzed for large and low values of the density ratio (Sect. 3).

2 Model problem

In an Euler flow, the evolution of the velocity gradient tensor, $\mathbf{A} = \nabla \mathbf{u}$, is described by the following equation:

$$\frac{DA_{ij}}{Dt} = -A_{i\alpha}A_{\alpha j} - \Pi_{ij}, \quad (1)$$

where the Π_{ij} 's are the components of the pressure Hessian tensor, $\Pi = \nabla[(\nabla p)/\rho]$, with p and ρ being respectively the pressure and the mass density.

In the two-dimensional case, Eq. (1) can be expressed by a four-equation system:

$$\frac{D\sigma_n}{Dt} = -\delta\sigma_n + \Pi_{22} - \Pi_{11}, \quad (2)$$

$$\frac{D\sigma_s}{Dt} = -\delta\sigma_s - \Pi_{12} - \Pi_{21}, \quad (3)$$

$$\frac{D\omega}{Dt} = -\delta\omega + \Pi_{12} - \Pi_{21}, \quad (4)$$

$$\frac{DP}{Dt} = -\frac{1}{2}(\sigma^2 - \omega^2 + P^2) - \Pi_{11} - \Pi_{22}, \quad (5)$$

where $\delta(t)$ is the expansion – or dilatation – rate, $\delta(t) = -1/\rho \cdot D\rho/Dt$, $\sigma_n = A_{11} - A_{22}$ and $\sigma_s = A_{12} + A_{21}$ are, respectively, the normal and shear components of strain, $\sigma = (\sigma_n^2 + \sigma_s^2)^{1/2}$ is the strain intensity, $\omega = A_{21} - A_{12}$ is the vorticity, and $P = A_{11} + A_{22}$ is the velocity divergence which – as a result of mass conservation – coincides with the dilatation rate: $P \equiv \delta$.

The model problem is based on assuming the expansion rate as:

$$\delta(c) = 4\delta_m c(1 - c), \quad (6)$$

with $c(t) = (\rho_o/\rho(t) - 1)/(\rho_o/\rho_\infty - 1)$ where $\rho_o \equiv \rho(0)$, and $\rho_\infty \equiv \lim_{t \rightarrow \infty} \rho(t)$; the density ratio is defined by ρ_o/ρ_∞ . The parabolic function modelling $\delta(c)$ is inspired from numerical simulation data for the velocity divergence across a flame front [7]. From the definitions of $c(t)$ and $\delta(t)$:

$$\frac{Dc}{Dt} = \left(c + \frac{1}{q}\right)\delta, \quad (7)$$

with $q = \rho_o/\rho_\infty - 1$. In this study, we state $\delta_m = q$, with $q > 0$, which means $\rho_\infty < \rho_o$ – and $\delta > 0$ – as a result, for instance, of heat release. Note that from the approach of Tien and Matalon [8] $\delta \simeq q/\tau_f$ in the reaction zone of a flame front, where τ_f is the flame timescale. Stating $\delta_m = q$ thus comes to normalize δ_m by $1/\tau_f$. This choice is convenient, for it makes $\delta(c)$ depend on a single parameter. Figure 1 shows $c(t)$ and $\delta(t)$ for $q = 5$ and $q = 1$.

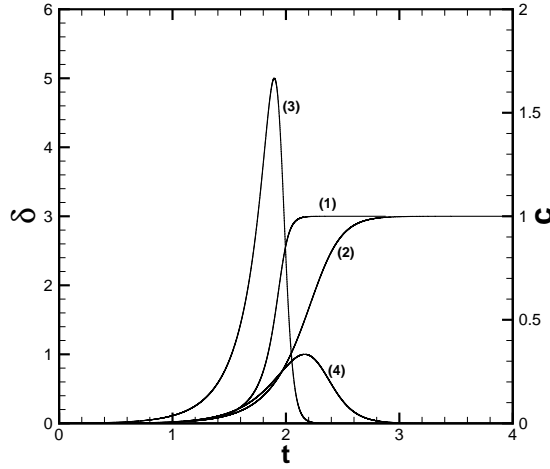


Fig. 1 Evolution of c and δ ; (1) $c(t)$ for $q = 5$; (2) for $q = 1$; (3) $\delta(t)$ for $q = 5$; (4) for $q = 1$

The evolution of the velocity tensor is computed from Eqs. (2)-(4), with the EHEE modelled equation for Π_{12} , Π_{21} , and Π_{22} [6]:

$$\frac{D\Pi_{ij}}{Dt} = -A_{\alpha j}\Pi_{i\alpha} - A_{\alpha i}\Pi_{\alpha j} - (n-1)A_{\alpha\alpha}\Pi_{ij}, \quad (8)$$

– in which n is the ratio of specific heats –, while component Π_{11} is computed from Eq. (5) with P derived from Eqs. (6) and (7).

A study spanning a range of initial conditions is not within the scope of this work. As a first step, the physical relevance of the model is checked with a single set of initial conditions, namely: $c(0) = 10^{-4}$, $\sigma_n(0) = -\delta_m$, $\sigma_s(0) = 0.1|\sigma_n(0)|$, $\omega(0) = \sigma(0)$, together with isotropy of tensor Π , namely $\Pi_{12}(0) = \Pi_{21}(0) = 0$, and $\Pi_{11}(0)$ and $\Pi_{22}(0)$ derived from Eq. (5) at $t = 0$, with $\Pi_{11}(0) = \Pi_{22}(0)$.

In Fig. 2, A_{11} , A_{22} and δ/A_{22} are plotted against c , for $q = 5$. Interestingly, the behaviour shown in Fig. 2 is akin to the structure of normal strain ($a_N \equiv A_{11}$) and tangential strain ($a_T \equiv A_{22}$) across a flame front [9, 7].

3 Effect of dilatation on strain structure

The evolution of strain tensor properties, namely strain eigenvalues, $\lambda_1 = (-\sigma + \delta)/2$ and $\lambda_2 = (\sigma + \delta)/2$ [10] as well as orientation of the strain eigenvectors, \mathbf{e}_1 and \mathbf{e}_2 , is examined for both $q = 5$ (large density ratio) and $q = 1$ (low density ratio) with the same latter initial conditions.

3.1 Large density ratio

Because it determines the sign of the lowest strain eigenvalue, the ratio of dilatation rate to strain intensity, δ/σ , is a significant parameter of the dynamics

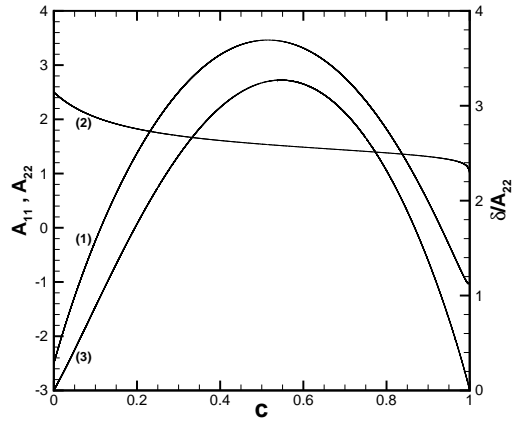


Fig. 2 Diagonal components of A, (1) A_{11} , (2) A_{22} ; (3) ratio δ/A_{22} , vs. c , for $q = 5$

of a scalar gradient in a non-solenoidal flow [10]. As shown in Fig. 3, dilatation makes the smallest eigenvalue, λ_1 , positive – which thus means two extensional strain directions – over most of the c -range, where $\delta/\sigma > 1$. It is only at the edges ($c < 0.12$, and $c > 0.92$), where $\delta/\sigma < 1$, that $\lambda_1 < 0$, which thus leads to one compressional and one extensional strain directions.

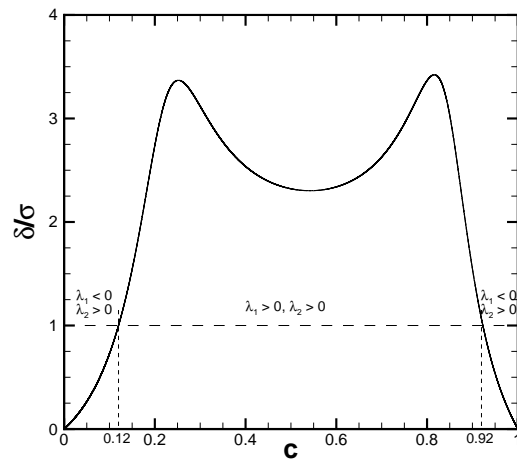


Fig. 3 Ratio δ/σ and sign of strain eigenvalues vs. c ; $q = 5$

The orientation of strain eigenvectors is shown by $\Phi = \arctan(\sigma_n/\sigma_s)/2 - \pi/4$, the angle between axis x_1 and the direction of the largest strain, e_2 (Fig. 4). For small c , $\Phi < -\pi/4$, which means that direction x_1 mostly undergoes the influence of the smallest strain. As c increases, counterclockwise rotation of strain axes brings the direction of the largest strain near x_1 , and this orientation is hold over the intermediate c -range. As c reaches the upper range, rotation of strain axes is reversed, and the direction of the lowest strain comes back close to x_1 . These changes in strain axes orientation, in particular, alignment of the largest strain with the direction of anisotropy, are consistent with the evolution of strain approaching a flame front [5,11].

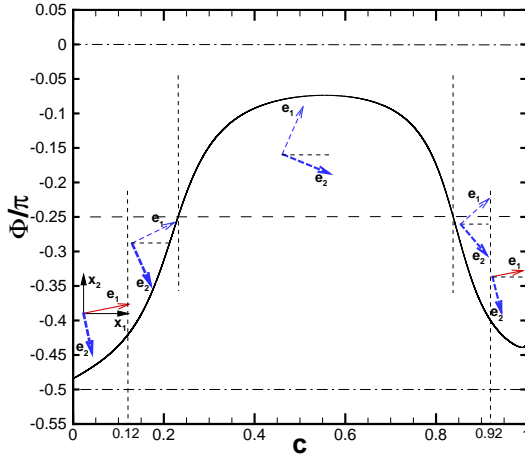


Fig. 4 Angle Φ between x_1 and the direction of largest strain, e_2 , vs. c ; $q = 5$; a solid arrow indicates compressional strain, while a dashed arrow indicates extensional strain; direction of the largest strain is shown by a bold dashed arrow

In this two-dimensional Euler flow, rotation of strain principal axes is promoted by anisotropy of the pressure Hessian tensor [12]. The rotation rate of strain eigenvectors is indeed given by $\Omega = 2D\Phi/Dt = \sigma^{-2}(\sigma_s D\sigma_n/Dt - \sigma_n D\sigma_s/Dt)$, and then, from Eqs. (2) and (3), $\Omega = \sigma^{-2}[\sigma_s(\Pi_{22} - \Pi_{11}) + \sigma_n(\Pi_{12} + \Pi_{21})]$. Figure 5 clearly shows the anisotropy of Π revealed by Π_{11} prevailing over the other components, and the resulting rotation rate, Ω .

3.2 Low density ratio

Similar features of strain evolution are retrieved for $q = 1$ with, however, a lesser influence of expansion rate. The lowest strain eigenvalue again gets positive for intermediate c values as expansion rate exceeds strain intensity, but this time over a somewhat shorter range (Fig. 6).

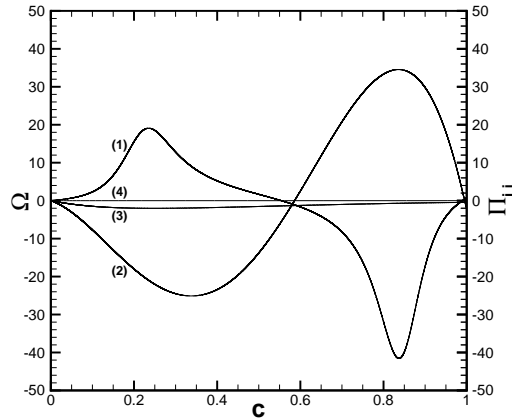


Fig. 5 Rotation rate of strain principal axes, Ω , and components of pressure Hessian tensor, Π_{ij} , vs. c ; $q = 5$; (1) Ω ; (2) Π_{11} ; (3) Π_{12} and Π_{21} ; (4) Π_{22}

The influence of density ratio is more obvious in strain axes orientation (Fig. 7). The direction of the largest strain comes much less close to x_1 over the intermediate c -range, and the latter is more narrow as well. This directly results from a weaker rotation rate, Ω , for $q = 1$ (not shown). Indeed the lower q , the smaller the respective magnitudes of strain components, σ_n and σ_s , and of anisotropic terms, $\Pi_{22} - \Pi_{11}$ and $\Pi_{12} + \Pi_{21}$; and the level of σ^{-2} – greater for $q = 1$ than for $q = 5$ – is not enough to balance this difference.

4 Conclusion

The mechanisms underlying the influence of dilatation on the velocity gradient tensor can be reliably addressed with a model problem. Assuming a likely evolution of the expansion rate, the solution of an equation system for the components of the velocity gradient and of the pressure Hessian includes a number of features regarding the evolution of the dynamic field as a density front is approached.

The ratio of dilatation rate to strain intensity, a critical parameter in the variable-mass-density kinematics of scalar gradient, is derived. More specifically, the evolution of normal and tangential strains is reminiscent of strain structure at the crossing of a flame front. Finally, the pressure Hessian anisotropy resulting from forcing the expansion rate promotes the rotation of strain principal axes, which subsequently aligns the largest strain with the direction of anisotropy, a result relevant to questions at issue in the physics of flames. Extension of the approach to the three-dimensional case as well as to the coupling of the velocity gradient dynamics with the physics of a reacting scalar gradient is a work in progress.

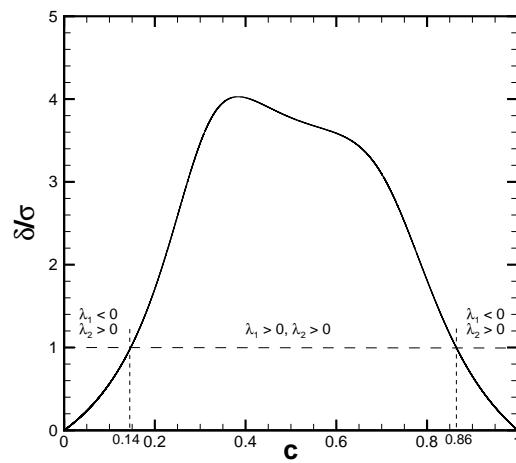


Fig. 6 Ratio δ/σ and sign of strain eigenvalues vs. c ; $q = 1$

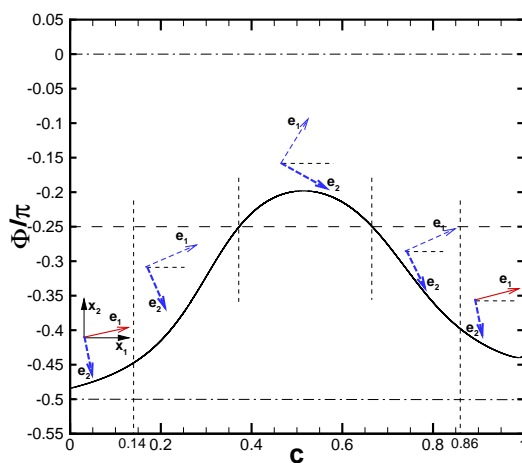


Fig. 7 Angle Φ between x_1 and the direction of largest strain, e_2 , vs. c ; $q = 1$; a solid arrow indicates compressional strain, while a dashed arrow indicates extensional strain; direction of the largest strain is shown by a bold dashed arrow

Conflict of interest statement

On behalf of all authors, the corresponding author states that there is no conflict of interest.

Acknowledgement

This is a post-peer-review, pre-copyedit version of an article published in Springer Nature Applied Sciences. The final authenticated version is available online at: <http://dx.doi.org/10.1007/s42452-020-03513-4>

References

1. Danish, M., Suman, S., Girimaji, S.S.: Influence of flow topology and dilatation on scalar mixing in compressible turbulence. *J. Fluid Mech.* **793**, 633-655 (2016)
2. Boukharfane, R., Bouali, Z., Mura, A.: Evolution of scalar and velocity dynamics in planar shock-turbulence interaction. *Shock Waves* **28**, 1117-1141 (2018)
3. Swaminathan, N., Grout, R.W.: Interaction of turbulence and scalar fields in premixed flames. *Phys. Fluids* **18**, 045102 (2006)
4. Dopazo, C., Cifuentes, L.: The physics of scalar gradients in turbulent premixed combustion and its relevance to modeling. *Combust. Sci. and Tech.* **188**, 1376-1397 (2016)
5. Zhao, S., Er-ray, A., Bouali, Z., Mura, A.: Dynamics and kinematics of the reactive scalar gradient in weakly turbulent premixed flames. *Combust. Flame* **198**, 436-454 (2018)
6. Suman, S., Girimaji, S.S.: Dynamical model for velocity-gradient evolution in compressible turbulence. *J. Fluid Mech.* **683**, 289-319 (2011)
7. Dopazo, C., Cifuentes, L., Martin, J., Jimenez, C.: Strain rates normal to approaching iso-scalar surfaces in a turbulent premixed flame. *Combust. Flame* **162**, 1729-1736 (2015)
8. Tien, J.H., Matalon, M.: On the burning velocity of stretched flames. *Combust. Flame* **84**, 238-248 (1991)
9. Chakraborty, N., Rogerson, J.W., Swaminathan, N.: The scalar gradient alignment statistics of flame kernels and its modelling implications for turbulent premixed combustion. *Flow Turbulence Combust.* **85**, 25-55 (2010)
10. Gonzalez, M., Paranthoën, P.: Effect of variable mass density on the kinematics of the scalar gradient. *Phys. Fluids* **23**, 075107 (2011)
11. Steinberg, A.M., Driscoll, J.F., Swaminathan, N.: Statistics and dynamics of turbulence-flame alignment in premixed combustion. *Combust. Flame* **159**, 2576-2588 (2012)
12. Lapeyre, G., Klein, P., Hua, B.L.: Does the tracer gradient align with strain eigenvectors in 2D turbulence? *Phys. Fluids* **11**, 3729-3737 (1999)